Aerodynamics Numerical Laboratory

3D Project: Weissinger

Department of Aerospace Science and Technology (DAER)
Professor: Luca Cortelezzi, Federico Ghioldi

Matricola	Last Name	First Name
225720	Schifone	Marco

POLITECNICO DI MILANO
Academic Year 2022-2023

December 15, 2022

Contents

List of Figures

List of Tables

1 Introduction

The main objective of the 3D project is to implement the method of Weissinger, in order to study the flow over a wing of finite span, then will be also studied the tandem configuration with the ground effect. In particular, we will have to modify the geometric characteristics of the wing, such as taper ratio, chord, dihedral angle, in order to match the required performance in terms of lift coefficient.
It is important to remember the assumptions that are made in order to describe the problem by means of the Weissinger method: the flow field is incompressible, inviscid and irrotational, the angle of attack needs to be small and the lifting surfaces are small as well.
In the Weissinger method a series of horseshoe vortices is used in order to reproduce the variation of circulation on the wing. As it happened in the Hess-Smith a discretization into panels will be necessary. If N is the number of panels along the chord, and $2M$ the number of panels in the spanwise direction, we will have $2M \times N$ panels, on which a vortex of constant strength is placed. The unknowns can be found by imposing the same number of boundary condition equations. Once the unknown circulation is computed, it is possible to determine the aerodynamic loads on the wing, in particular we are interested in the pressure, lift and induced drag coefficient, as well as the pitching moment.
The main difference with the Hess-Smith method is that now we are dealing with a 3D geometry, so now we have to consider the effects of the tip vortices produced due to the difference of pressure between the bottom and top surface of the wing. This will imply the presence of an induced angle of attack, and the presence of a resultant induced drag generated as well as the reduction in the total lift produced.
The validation of the code will be provided by means of the use of the program XFLR5, in particular we will investigate the error in the lift coefficient in the spanwise direction. It is important to notice that in the Weissinger method we are considering the wing as a plate of null thickness, whereas in XFLR5 it is necessary to define an airfoil in order to analyze the problem. Then, the airfoil NACA 0006 will be chosen because of its symmetry and also because of the small value of the maximum thickness. The only two data of the problem are presented in Table 1.

$$\alpha_w \quad = \quad 2\,^\circ \;\Big|\; c_L \quad = \quad 0.3 \pm 0.05$$

Table 1: Data of the problem.

2 Numerical Analysis

2.1 Single wing configuration

In order to match the lift coefficient required, it necessary to evaluate the effects of the wing geometry (taper ratio λ, dihedral angle d, sweep angle Λ) on the performance of the wing itself. Then we will investigate how the c_L changes with both λ, Λ as the angle of attack varies. From the results shown in Figure 1, 2 it is possible to notice that the effects on the lift coefficient are opposite. The increase in the taper ratio is linked to an increase in both the lift produced at the same angle of attack and in the induced drag coefficient c_{Di}. Moreover, an increase in the sweep angle generates a decrease in both the lift and induced drag coefficients.
Then, by taking into account the results of this simple analysis, it is possible to compute the lift coefficient of the wing in different configurations.

Root chord c_R	Tip chord c_T	Wing span b	Sweep angle Λ	Dihedral angle d	c_L
1.6 m	1.1 m	11 m	0 °	0 °	0.1669
1.6 m	1.1 m	11 m	10 °	2 °	0.1628
1.6 m	1.1 m	22 m	10 °	2 °	0.1863
2.25 m	1 m	25 m	10 °	2 °	0.1881

Table 2: Lift coefficient for different configurations

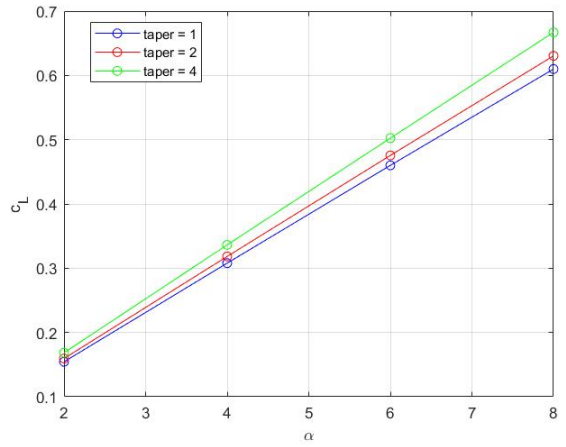

Figure 1: Taper ratio effect on the lift coefficient

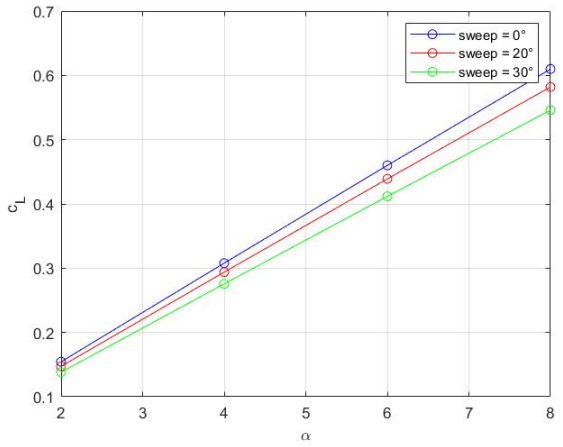

Figure 2: Sweep angle effect on the lift coefficient

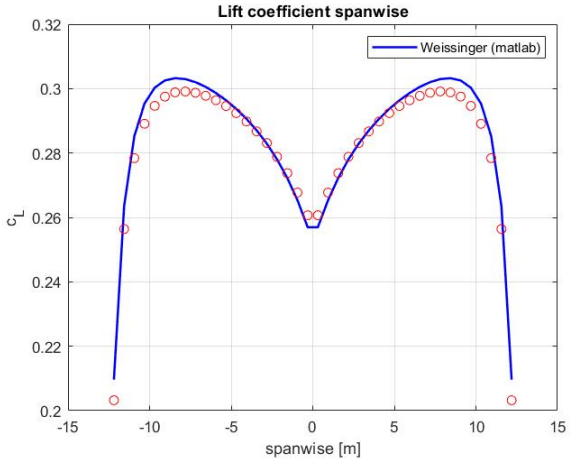

Figure 3: Spanwise lift coefficient

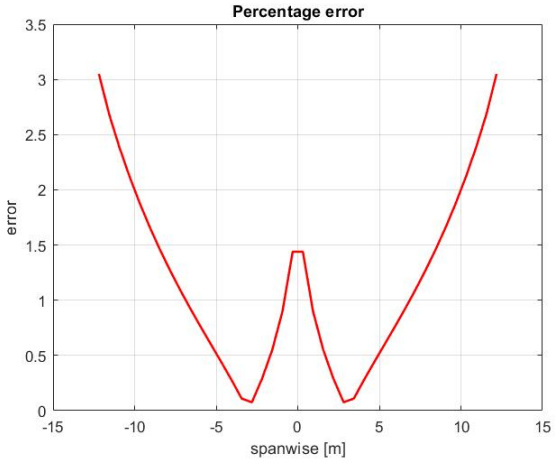

Figure 4: Percentage error on the lift coefficient

From the results shown in Table 2 it is possible to notice how the c_L changes with different configurations, but with the given angle of attack it is very difficult to approach the value of the lift coefficient required. Then, by considering the configuration 4, we will change the angle of attack to $\alpha_w = 3°$, in order to match the requirement in terms of lift coefficient. As a matter of fact, the resultant lift coefficient is $c_L = 0.2819$. Now it is necessary to validate the code by means of the program XFLR5 with the configuration that has just been described, the results are shown in Figure 3, 4, from which we can notice that the error is always under the 3%, so this approximation can be considered acceptable for our analysis. The results in terms of lift, induced drag and pitching moment coefficients are shown below in Table 3.

Lift coefficient c_L	Induced drag coefficient c_{Di}	Pitching moment coefficient c_M
0.2819	0.0148	-0.1745

Table 3: Coefficients for the wing only configuration

2.2 Tandem configuration

Now we will investigate the tandem configuration, by introducing an horizontal tail with the following geometric characteristics, presented in Table 4, in order to validate our code. Then these parameter will be changed with the purpose of minimizing the pitching moment with respect to the leading edge

of the wing. The tail is located at a given horizontal distance of $x_{1,2} = 5\,\text{m}$ and a vertical distance of $y_{1,2} = 0.5\,\text{m}$ both measured from the leading edge of the wing to the leading edge of the tail.

$\alpha_w = 3°$	$c_{R,wing} = 2.25\,\text{m}$	$c_{T,wing} = 1\,\text{m}$	$b_{wing} = 25\,\text{m}$	$\Lambda_w = 10°$	$d_w = 2°$
$\alpha_t = 3°$	$c_{R,tail} = 1.5\,\text{m}$	$c_{T,tail} = 1.5\,\text{m}$	$b_{tail} = 6\,\text{m}$	$\Lambda_t = 0°$	$d_t = 0°$

Table 4: Geometric characteristic of the tandem configuration

It is possible to extend our code in order to analyze the tandem configuration by slightly changing it, by introducing the mutual effects between wing and tail, similarly to what has been done in the Hess-Smith method. The unknowns of the problem are now increasing to $2N_w \times M_w + 2N_t \times M_t$, which are evaluated by imposing no-penetration boundary condition on all the panels' control points. The results of the analysis are shown in Figure 5, 6, from which we can see that again the error is under the 3.5%, which is still acceptable and the code can be considered valid also for the tandem configuration.

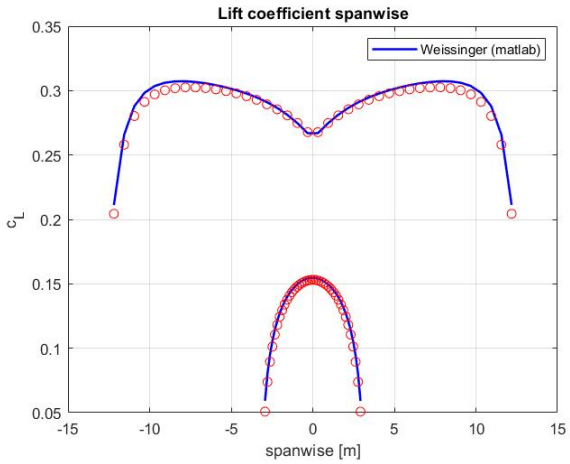

Figure 5: Lift coefficient for the tandem configuration

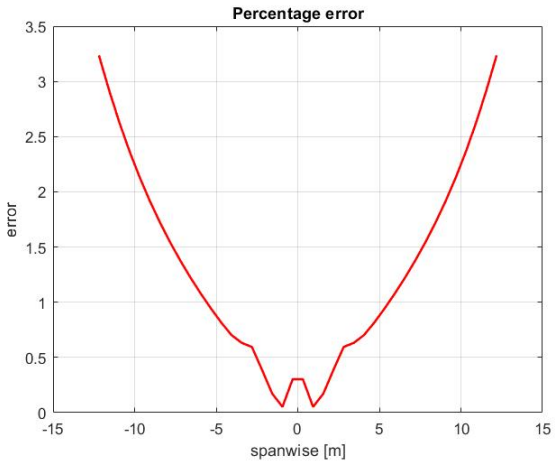

Figure 6: Percentage error on the lift coefficient of the wing

Now we have to change the geometric characteristics of the tail in order to minimize the pitching moment but by maintaining the lift coefficient of the wing as $c_{L,wing} = 0.3 \pm 0.05$. We will keep the same angle of attack α_t and both the horizontal and vertical distance from the wing, in order to investigate only the effects of the geometry of the tail.

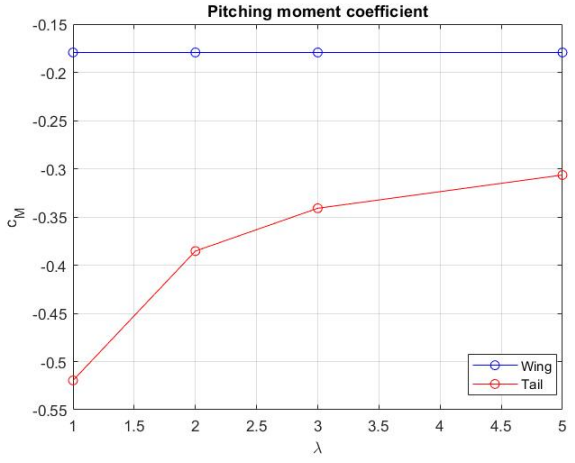

Figure 7: Pitching moment coefficient as taper ratio changes

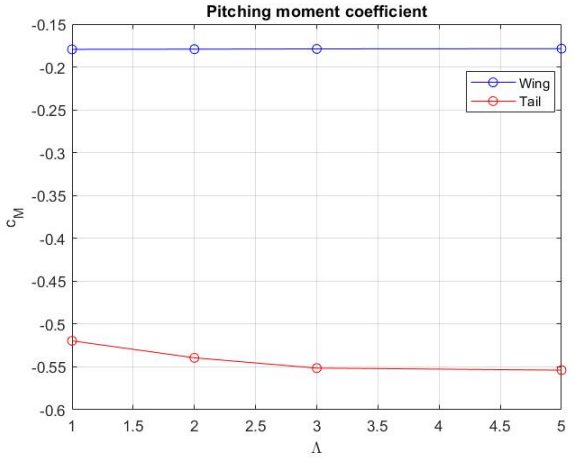

Figure 8: Pitching moment coefficient as Λ changes

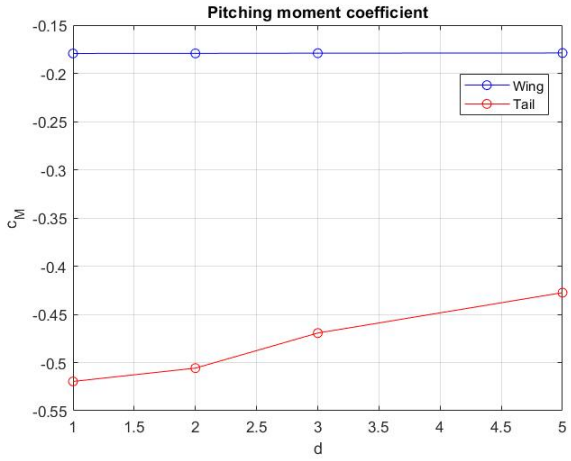

Figure 9: Pitching moment coefficient as dihedral angle changes

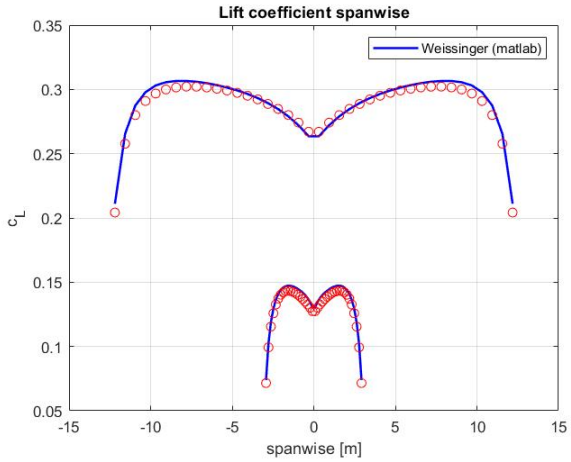

Figure 10: Lift coefficient for wing and tail, configuration 2

The results of the analysis are shown in Figure 7, 8, 9, from which it is possible to notice that the geometry of the wing in terms of taper ratio, sweep angle and dihedral angle has a very slight influence in the pitching moment coefficient of the main wing, whereas the one tail is much more affected. Moreover the effect of both the taper ratio and the dihedral angle is to reduce the pitching moment, with the first that has a greater influence. On the other hand the increase in the sweep angle Λ causes an increase in the pitching moment of the tail. With the chosen configuration, with the data presented in Table 5, the lift coefficient of the wing and the tail is shown in Figure 10, where are always present the numerical results coming from XFLR5. The results of the analysis of the tandem configuration are presented in Table 6.

$\alpha_w = 3°$	$c_{R,wing} = 2.25\,\text{m}$	$c_{T,wing} = 1\,\text{m}$	$b_{wing} = 25\,\text{m}$	$\Lambda_w = 10°$	$d_w = 2°$
$\alpha_t = 3°$	$c_{R,tail} = 2\,\text{m}$	$c_{T,tail} = 1\,\text{m}$	$b_{tail} = 6\,\text{m}$	$\Lambda_t = 10°$	$d_t = 3°$

Table 5: Geometric characteristic of the tandem configuration

$c_{L,wing}$	$c_{L,tail}$	$c_{Di,wing}$	$c_{Di,tail}$	$c_{M,wing}$	$c_{M,tail}$
0.2867	0.1323	0.0150	0.0069	-0.1772	-0.4021

Table 6: Coefficients for the tandem configuration

2.3 Tandem configuration with ground effect

Now we have to consider the influence of the ground effect on the tandem configuration, again it will be necessary to introduce some slightly changes in the code. Similarly to what has been done in the Hess-Smith method, it is necessary to use the method of images in order to evaluate how the ground effect affects the performance of the wing and the tail. Since the vortices on the mirrored wings have the same strength of the vortices on the real wings, the number of unknowns is again $2N_w \times M_w + 2N_t \times M_t$, which are evaluated by imposing no-penetration boundary condition on all the panels' control points.

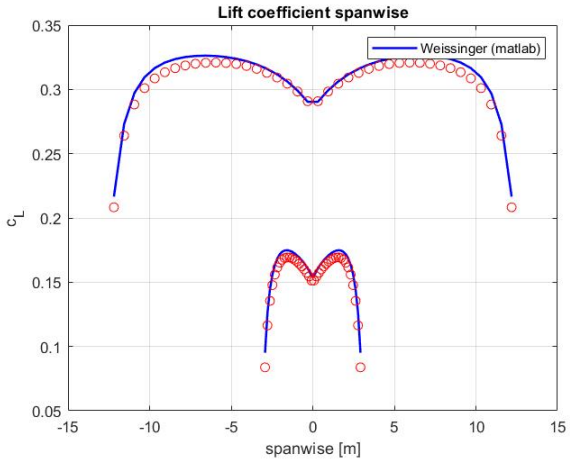

Figure 11: Lift coefficient for tandem configuration with ground effect.

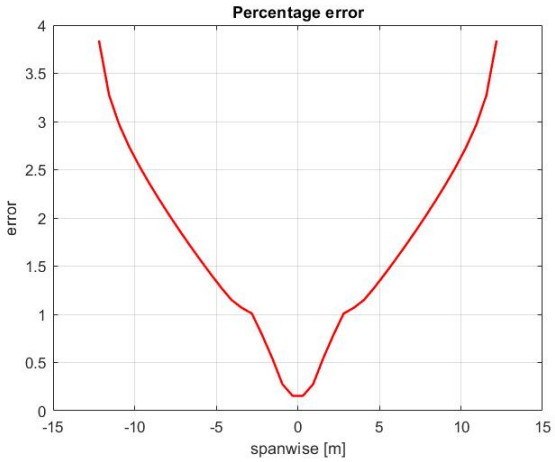

Figure 12: Percentage error on the lift coefficient of the wing.

For this analysis we are considering the distance h from the ground, which is $h = 3\,\text{m}$. The results of the analysis are shown in Figure 11, 12. Then we can evaluate the lift coefficient for wing and tail, as well as the induced drag coefficient, the results are presented in the Table 7. As expected the lift coefficient as well as the induced drag coefficient for both the wing and the tail is higher compared to the values that were found for the tandem configuration without the influence of the ground effct.

$c_{L,wing}$	$c_{L,tail}$	$c_{Di,wing}$	$c_{Di,tail}$
0.3056	0.1694	0.0160	0.0089

Table 7: Coefficients for the tandem configuration with ground effect.